FROM PHASE TRANSITIONS TO CHAOS

TOPICS IN MODERN STATISTICAL PHYSICS

Edited by

Géza Györgyi
Imre Kondor
László Sasvári
Tamás Tél

Institute for Theoretical Physics
Eötvös University, Budapest
Hungary

World Scientific (1992)
Singapore • New Jersey • London • Hong Kong

1D RANDOM FIELD ISING MODEL AND NONLINEAR DYNAMICS

ULRICH BEHN and ADRIAN LANGE
Sektion Physik der Universität Leipzig
Augustusplatz 10, O-7010 Leipzig, Germany

ABSTRACT

The one-dimensional random field Ising model (1D RFIM) is related to a nonlinear discrete stochastic mapping for an effective local random field which has for nonzero temperature a multifractal measure which may be thin or fat. By means of symbolic dynamics we distinguish parameter regions where the measure at the boundary of the support diverges or goes to zero with infinite or zero slope, respectively. Within the thermodynamic formalism we calculate generalized fractal dimensions as function of physical parameters.

1. Introduction

The calculation of the partition function of the one-dimensional Ising model in a quenched random magnetic field h_n can be reduced to the problem of *one* spin in an effective local random field ξ_N[1,2]

$$Z^N = \sum_{\{s_n\}} \exp\Big(\beta \sum_{n=1}^{N-1} J s_n s_{n+1} + \sum_{n=1}^{N} h_n s_n\Big) = \sum_{s_N} \exp\Big[\beta\Big(\xi_N s_N + \sum_{n=1}^{N-1} B(\xi_n)\Big)\Big] \tag{1.1}$$

by summing up the left-most spin of the chain. The effective local random field ξ_n acting on s_n is governed by the discrete stochastic mapping[2]

$$\xi_n = h_n + A(\xi_{n-1}) \equiv f(h_n, \xi_{n-1}), \qquad \xi_0 = 0;\ n = 1, \ldots, N, \tag{1.2}$$

where

$$\begin{aligned} A(x) &= (2\beta)^{-1} \ln[\cosh\beta(x+J)/\cosh\beta(x-J)], \\ B(x) &= (2\beta)^{-1} \ln[4\cosh\beta(x+J)\cosh\beta(x-J)]. \end{aligned} \tag{1.3}$$

We consider a random field h_n which can take only two values $h_\pm = h_0 \pm h$ with the same probability $\frac{1}{2}$ and is on each lattice site independent and identically distributed. (The generalization to correlated Markov chains is straightforward). The mapping (1.2) induces in the nth step a probability density $p_n(x)$ for the

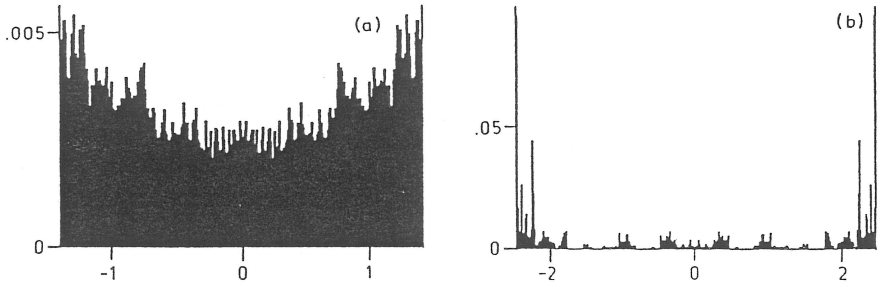

Figure 1. Distribution of the local magnetization generated by digital simulation ($kT = 1$, $J = 1$, $h_0 = 0$). The multifractal may be fat (a) or thin (b) for $h = 0.6$ and 1.5, respectively.

effective random field ξ_n governed by the Frobenius-Perron equation

$$p_n(x) = \int dx'\, p_{n-1}(x') \tfrac{1}{2} \sum_{\sigma=\pm} \delta(x - f(h_\sigma, x')). \tag{1.4}$$

The fixed point of Eq. 1.4 gives the invariant measure of the local random field which can be used to calculate physical quantities like free energy, magnetisation, or the Edwards-Anderson parameter[2]. The model allows some exact results and displays already general features of random field problems (see, e.g., Ref. 3), including frustration.

The properties of the discrete stochastic mapping — which is interesting of its own — depend on the nature of the driving process h_n and on the shape of the function A.

For non-zero temperatures $A(x)$ is infinitely differentiable and $|\partial_x A(x)| < 1$. As a consequence, the dynamics defined by Eq. 1.2 is *nonchaotic* in the sense that the averaged Lyapunov exponent is negative but the map generates for a discrete driving process an *uncountable* number of states and a fractal (strange) attractor. Due to the nonlinearity of $A(x)$ the mapping has infinitely many scales, and the invariant measure constitutes a *multifractal* which may be *fat* (the support is continuous) or *thin* (the support is fractal) depending on the physical parameters[4–11]. In the latter case the support has the topology of the Cantor set but it is *not* self-similar except for small values of the magnetic field or for high temperature where $A(x)$ is well approximated by a linear function. For a continuous driving process (without gaps) the support is always the continuum[5,6].

The multifractal properties of the effective field transfer directly to a physical quantity like local magnetisation (cf. Fig. 1) which could be measured in Mössbauer or NMR experiments. It is given by[2] $m_n = \tanh\beta[\xi_n + A(\xi'_{n+1})]$, where ξ'_n is generated by summing up the spins from the right end of the chain.

For zero temperature, $A(x)$ is piecewise linear with parts where $\partial_x A(x) = 0$. As a consequence, Eq. 1.2 generates for a discrete driving process only a *countable* number of states which is finite or infinite for rational or irrational ratio of exchange and magnetic field, respectively[8,12,13]. In the former case the theory of finite Markov chains[14] can be applied to determine the invariant measure[8,13].

The drastic changes in the quality of the measure and its support are naturally reflected in the behaviour of the generalized fractal dimensions D_q[15,16] which undergo, as function of the physical parameters, continuous as well as discontinuous transitions, similar to order parameters in phase transitions[4,7–10].

Furthermore, there is a close relation of the multifractal spectrum with the fluctuations of the free energy of a finite chain[10a,11].

In this paper we show that the parameter space is divided in regions where the invariant measure has qualitatively different shapes (Section 2). The analysis is based on an explicit representation of the measure[8b] summing up contributions for all possible trajectories which are encoded by symbolic dynamics[16]. In Section 3 we calculate generalized fractal dimensions as function of physical parameters including the case of nonvanishing average field. For parameters where the fractal is fat we have to reorganize the partition to take properly into account the contribution from overlapping bands.

2. Symbolic Dynamics and Qualitative Shape of the Invariant Measure

For non-zero temperature $A(x)$ is infinitely differentiable. Therefore, the result of an iteration of the mapping (1.2) and its associate Frobenius-Perron equation, Eq. 1.4, is uniquely determined by the realization of the quenched random field h_n. This allows to introduce a symbolic dynamics[8a,b] which encodes all states generated by Eq. 1.2 and all bands generated by Eq. 1.4 by the sequence of signs characterizing the random field, i.e., the *history* of the dynamical system.

We denote the result of the nth iteration of Eq. 1.2 starting from the initial value $\xi_0 = y$ by

$$x_{\{\sigma\}_n, y} = f(h_n, f(h_{n-1}, \ldots, f(h_1, y)\ldots)), \tag{2.1}$$

where $\{\sigma\}_n = \{\sigma_n, \ldots, \sigma_1\}$ is the sequence of signs corresponding to the given realization of the driving process $\{h_{\sigma_n}, \ldots, h_{\sigma_1}\}$. The result of infinitely many iterations is denoted by $x_{\{\sigma\}}$ where $\{\sigma\}$ symbolizes an infinite sequence of signs. It does not depend on the initial value y since $|\partial_x f(h, x)| < 1$ — the dynamics is *nonchaotic*.

The attractor of Eq. 1.2 which constitutes the support of the invariant measure lies on the interval $I = [x_{\{-\}}, x_{\{+\}}]$ bounded by the fixed points for infinitely many iterations with the upper or lower branches of the mapping, corresponding to constant fields h_+ or h_-, respectively,

$$x_{\{\sigma\}} = h_\sigma/2 + (2\beta)^{-1} \sinh^{-1}[e^{2\beta J} \sinh\beta h_\sigma], \quad \sigma = \pm \tag{2.2}$$

For parameters for which the two branches do *not* overlap, (cf. Fig. 2), the images of the interval $I_\sigma = [x_{\sigma\{-\}}, x_{\sigma\{+\}}]$, where $\sigma = \pm$, leave a first gap in the support $\Delta = [x_{-\{+\}}, x_{+\{-\}}]$ which generates in the nth iteration 2^n gaps,

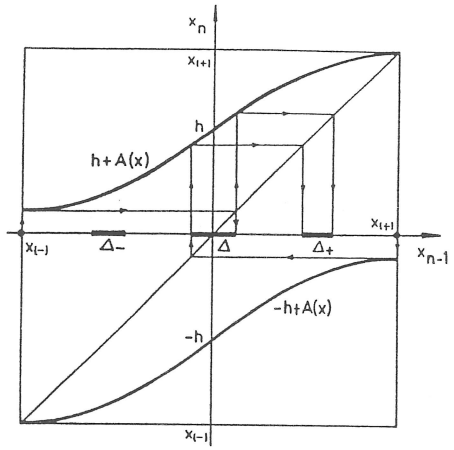

Figure 2. Mapping (1.2) for a parameter setting which gives a thin multifractal ($kT = 1$, $J = 1$, $h_0 = 0$, $h_1 = 1.2$). Shown are the fixed points $x_{\{\pm\}}$, the gap Δ and its first iterations $\Delta_\pm$.

$\Delta_{\{\sigma\}_n} = [x_{\{\sigma\}_n-\{+\}}, x_{\{\sigma\}_n+\{-\}}]$ which are arbitrarily close to a state. (Two states $x_{\{\sigma\}_n\{\sigma\}}$ and $x_{\{\sigma\}_n\{\sigma'\}}$ are the closer the longer is the *head* $\{\sigma\}_n$ which coincides).

Thus for $L_\Delta = x_{+\{-\}} - x_{-\{+\}} > 0$ the *support* is a fractal. $L_\Delta = 0$ defines a phase boundary in the parameter space (cf. Fig. 3). For $h_0 = 0$ the corresponding critical field is[8b]

$$h_c^{(1)} = (2\beta)^{-1} \cosh^{-1}[(e^{2\beta J} - 1)/2]. \tag{2.3}$$

With increasing h_0 the overlapping region changes as shown in Fig. 3b.

The iteration of the Frobenius-Perron equation, starting with a normalized initial measure $p_0(x)$ which is nonzero on I, yields in the nth iteration 2^n bands which can be uniquely encoded by symbolic dynamics, too. To evaluate the first iteration of (1.4) we exploit that $x_{\sigma,y} = f(h_\sigma)$ has the monotonic inverse

$$y_{\sigma,x} = f^{-1}(h_\sigma, x) = (2\beta)^{-1} \ln[\sinh\beta(J + x - h_\sigma)/\sinh\beta(J - x + h_\sigma)] \tag{2.4}$$

so that $\delta(x - f(h_\sigma, x')) = |\partial_{x'} f(h, x')|^{-1} \delta(x' - f^{-1}(h, x))$. The prefactor of the δ-function is calculated as $W(x') = |[\cosh(2\beta x') + \cosh(2\beta J)]/\sinh(2\beta J)|$ which gives for $x' = y_{\sigma,x}$

$$W(y_{\sigma,x}) = |\sinh(2\beta J)/[2\sinh\beta(J - x + h_\sigma)\sinh\beta(J + x - h_\sigma)]|. \tag{2.5}$$

Thus, Eq. 1.4 tells us that $p_0(x)$ generates two bands $p_\sigma(x)$, $\sigma = \pm$ living on the mappings of the initial support I_σ,

$$p_1(x) = \begin{cases} (1/2)p_0(y_{\sigma,x})W(y_{\sigma,x}) \equiv p_\sigma(x) & \text{for } x \in I_\sigma,\ \sigma = \pm, \\ 0 & \text{otherwise.} \end{cases} \tag{2.6}$$

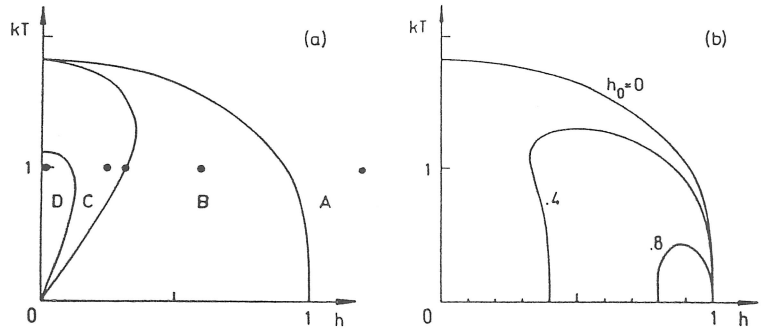

Figure 3. Parameter regions with qualitative different shape of the invariant measure ($J = 1$). Fig. 3a shows for $h_0 = 0$ the regions where the measure is a thin (A) or a fat (B, C, D) multifractal. At the boundaries of the support the measure may be infinite (A, B) or zero with infinite (C) or zero (D) slope. For given temperature the critical magnetic fields are given by Eqs. 2.3, 2.12, and 2.15, respectively. The dots indicate the parameters for which the measure is shown in Fig. 4. Fig. 3b shows for several values of h_0 the line $L_\Delta = 0$ separating the regions of fat and thin multifractals. (For $T = 0$ or $h = 0$ the measure lives on a countable number of points).

A band $p_{\{\sigma\}_{n-1}}(x)$ living on $I_{\{\sigma\}_{n-1}}$ generates in the next iteration the two bands

$$p_{\{\sigma\}_n}(x) = \tfrac{1}{2} p_{\{\sigma\}_{n-1}}(y_{\{\sigma\}_n,x}) W(y_{\sigma_n,x}), \quad x \in I_{\{\sigma\}_n}, \tag{2.7}$$

where $y_{\{\sigma\}_n,x}$ denotes a branch of the nth inverse:

$$y_{\{\sigma\}_n,x} = f^{-1}(h_1, f^{-1}(h_2, \ldots, f^{-1}(h_n, x)\ldots)). \tag{2.8}$$

From Eqs. 2.6 and 2.7 we obtain the closed expression[8b]

$$p_{\{\sigma\}_n}(x) = p_0(y_{\{\sigma\}_n,x}) \prod_{\nu=1}^{n} [\tfrac{1}{2} W(y_{\{\sigma\}_\nu,x})], \quad x \in I_{\{\sigma\}_n}. \tag{2.9}$$

The measure in the nth generation consists of 2^n bands $p_{\{\sigma\}_n}(x)$ labeled by the 2^n possible configurations $\{\sigma\}_n$ which contribute only if the argument x lies in the corresponding image of the initial support $I_{\{\sigma\}_n} = [x_{\{\sigma\}_n\{-\}}, x_{\{\sigma\}_n\{+\}}]$

$$p_n(x) = \sum_{\{\sigma\}_n} p_{\{\sigma\}_n}(x). \tag{2.10}$$

This is the analogue of a functional integral representation of the measure summing up contributions for all possible trajectories. The explicit expression (2.9) is helpful to investigate the qualitative behaviour of the measure and to calculate generalized scaling exponents.

The behaviour of the measure at the boundary of its support can be analyzed by exploiting that the preimage of the fixed point is the fixed point itself. For

example we consider the right boundary $x_{\{+\}}$. In the nth iteration we obtain from Eq. 2.9 for the rightmost band

$$p_{\{+\}_n}(x_{\{+\}}) \propto [\tfrac{1}{2}W(x_{\{+\}})]^n. \tag{2.11}$$

In the limit $n \to \infty$ the condition $W(x_{\{+\}}) = 2$ separates two parameter regions in which the invariant measure at its right boundary diverges or goes to zero, respectively, (cf. Fig. 3a). The corresponding critical magnetic field is

$$h_c^{(2)} = \tfrac{1}{\beta}\sinh^{-1}[2^{-3/2}(9e^{-4\beta J} + e^{4\beta J} - 10)^{1/2}(e^{4\beta J} - 1)^{-1/2}]. \tag{2.12}$$

In a similar way, for the derivative of the rightmost band at the right boundary we calculate from Eq. 2.9

$$\partial_x p_{\{+\}_n}(x)\Big|_{x=x_{\{+\}}} \propto \Big[(\tfrac{1}{2})^n W(x)^{n-1}\partial_x W(x)\prod_{\nu=1}^{n}(\partial_x y_{+,x})^\nu\Big]_{x=x_{\{+\}}} \tag{2.13}$$

which gives in the limit $n \to \infty$ the condition $W(x)\partial_x y_{+,x} = 2$, where $x \equiv x_{\{+\}}$, separating two parameter regions in which the derivative of the invariant measure at its right boundary diverges or goes to zero, respectively, (cf. Fig. 3a). With Eq. 2.5 and

$$\partial_x y_{+,x} = \sinh(2\beta J)/\{\cosh(2\beta J) - \cosh[2\beta(x - h_+)]\} \tag{2.14}$$

we obtain the corresponding critical magnetic field

$$h_c^{(3)} = \tfrac{1}{\beta}\sinh^{-1}[3\cdot 2^{-5/2} - 1/2 - (3\cdot 2^{-5/2} + 1/2)e^{-4\beta J}]^{1/2}. \tag{2.15}$$

These qualitative changes of the invariant measure are illustrated for typical parameters in Fig. 4.

3. Generalized Fractal Dimensions

The multifractal invariant measure may be characterized by generalized fractal dimensions[16]

$$D_q = \frac{1}{q-1}\lim_{l\to 0}\frac{\ln\sum_i^{N(l)} P_i^q}{\ln l}, \tag{3.1}$$

where l is the size of the $N(l)$ bins and P_i the total weight of the measure on bin i. (It is tacitely assumed to restrict the sum to non-empty bins). The parameter q can take continuous values, D_0 is the Hausdorff dimension of the support, D_1 and D_2 are the information and the correlation dimension, respectively. $D_{-\infty}$ and D_∞ characterize the most rarified (non-empty) part of the measure and give (D_q is monotonously decreasing with increasing q) the width of the multifractal spectrum which is for the 1D RFIM directly related to the fluctuations of the free energy[10a].

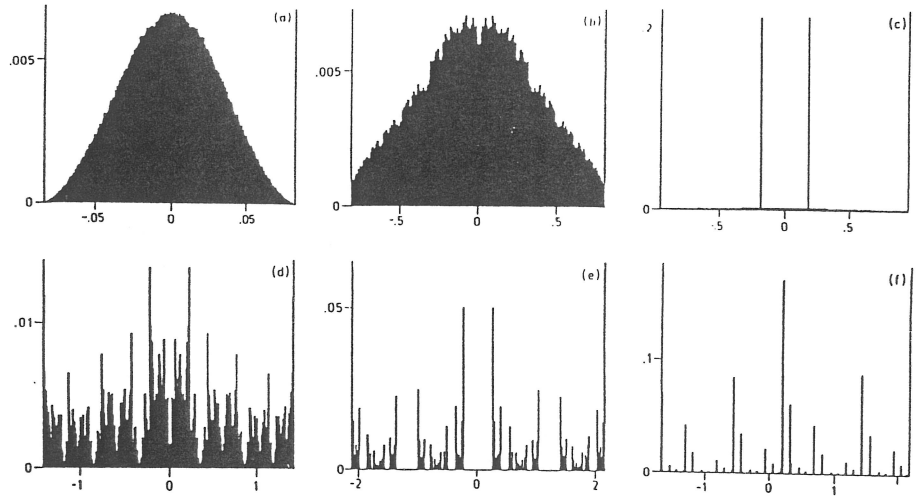

Figure 4. Qualitative different shape of the invariant measure. In Figs. 4a-e we have $kT = 1$, $h_0 = 0$, $J = 1$ and in consecutive order $h = 0.02, 0.25, 0.3177, 0.6$ and 1.2. For small h and kT not too large (Fig. 4a) the singularities of the measure gradually die out and it is near to a Gaussian, cf. also Ref. 4a. Fig. 4f where $kT = 0.15$, $h_0 = 1/4$, $h = 1$, $J = 15/16$ is already very near to the result for the groundstate (cf. Fig. 2 in Ref. 8b). The histograms are generated by digital simulation of $10^5 \ldots 10^7$ trajectories. (Note the different scales on both abscissas and ordinates).

In a *one-scale* approximation all D_q are equal and can be analytically calculated. It is justified for weak disorder or high temperature and reproduces — in a mean slope approximation— the correct size of the first gap[8a] .

An efficient tool to calculate the fractal dimensions is to consider an associated *repeller* problem[17]. Compensation of the local escape rate (depending on the fractal dimension) leads to a generalized Frobenius-Perron equation which becomes stationary if the fractal dimension was correctly chosen. This was applied to calculate D_0 for the 1D RFIM both numerically and by perturbation theory[7], and later elaborated to obtain the full spectrum of D_q[9]. The idea to make a generalized Frobenius-Perron equation stationary works also for attractors[18–20] and is used to study multifractal characteristics of a random map in the contribution by C. van den Broeck and T. Tél in this volume. Another method conceives the stochastic mapping (1.2) as the backward iteration of a deterministic map and relates D_q to non-natural measures[10].

It is advantageous to use instead of the equipartition of the support in identical bins of size l as in Eq. 3.1 a *natural* partition $\{l_i\}$ generated by the mapping itself. In the thermodynamic formalism[15] one introduces a partition function

$$\Gamma(\{l_i\}, q) = \sum_{\{l_i\}}\frac{P_i^q}{l_i^\tau}, \tag{3.2}$$

which goes with increasing resolution of the partition to infinity or to zero unless

$\tau = (q-1)D_q$. This can be used to determine D_q. It can be shown that the dimensions in Eqs. 3.1 and 3.2 are the same[16].

For parameters where the multifractal is *thin* the intervals of the natural partition in the nth iteration of Eq. 1.2 are the 2^n images $I_{\{\sigma\}_n}$ of the initial interval I which are disjoint and carry each the same measure $(1/2)^n$. A naive extrapolation of this partition into the region where the two branches of the map do overlap would give spurious results, e.g., D_q for $q \geq 0$ could increase its upper bound 1.

For parameters where the multifractal is *fat* the $I_{\{\sigma\}_n}$ overlap. The support is now the whole interval I which is naturally partitioned by the 2^{n+1} images $x_{\{\sigma\}_n\{\pm\}}$ of the fixed points $x_{\{\pm\}}$ in $(2^{n+1}-1)$ non-intersecting new intervals. Each of the new intervals may carry weight coming partially from several bands $p_{\{\sigma\}_n}(x)$. These bands are explicitly given by Eq. 2.9 so that their contribution can be properly taken into account.

There exist several concepts to characterize fat fractals[21], a detailed comparison is however beyond the scope of this paper. Very recently, the standard multifractal formalism was modified to describe multi-affine functions[22].

We calculated the partition function, Eq. 3.2, for the natural partitions described above generated in the nth and $(n+1)$st iteration and used $\Gamma_{n+1} - \Gamma_n = 0$, $(n = 8 \ldots 13)$ as eigenvalue equation to determine D_q $(q = -1, 0, 1, 2)$ as function of physical parameters allowing $h_0 \neq 0$ (cf. Fig. 5).

We also looked for $D_{\pm\infty}$. The kneading sequences leading to the most rarified and most concentrated part of the measure, which are for $h_0 = 0$ $\{-+\}$ and $\{+\}$, respectively[9], depend for $h_0 > 0$ on the value of h. We found for instance for $kT = 3.5$ and $h_0 = .8$ that the most rarified region for large h is generated by $\{-+\}$ and for small h by $\{-\}$. This may announce some transition which deserves further investigation.

4. Concluding Remarks

Symbolic dynamics turns out to be also useful for the study of correlation functions. The decay rates are given by *local* Lyapunov exponents.

Especially interesting is the limit of zero temperature where the uncountable number of states collapses to a countable number[8a,b,13]. The groundstate of the 1D RFIM may be macroscopically degenerated even for a continuous range of parameters[13]. The lines in the parameter space where the bands overlap end at $T = 0$ in critical parameters where the residual entropy has spikes and spin clusters flip[4a,8b,c].

The discrete mapping can be slightly modified to study the RFIM on a Bethe lattice[23]. For certain parameter ranges the measure is also fractal.

Mappings similar to Eq. 1.2 appear naturally also in different context, e.g., for a Schrödinger equation with random potential[24a], in cellular automata[24b], or as learning rules for forgetful memories[24c]. For the latter problem an analysis similar to the one presented here can be performed[25].

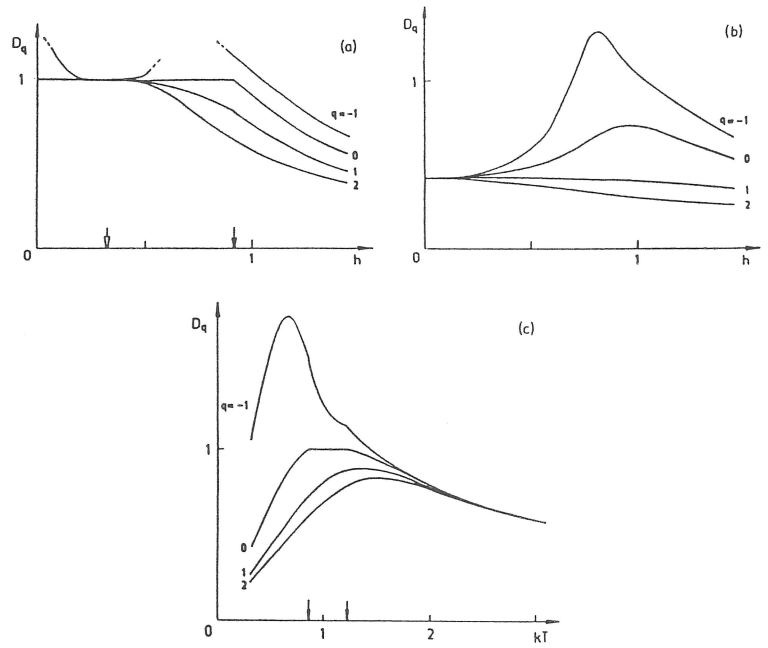

Figure 5. Generalized fractal dimensions of the invariant measure. The solid arrows in (a) and (c) indicate the parameters for which the gap vanishes (cf. Fig. 3b). For $kT = 0$ or $h = 0$ the measure lives on a countable set of points for which $D_0 = 0$. There are discontinuous, (a) and (b), as well as smooth (c) transitions. For small field (b) or high temperature (c) the width of the multifractal spectrum shrinks to zero and a one-scale approximation is appropriate. Near the critical parameter where the measure at the boundary of the support changes from infinity to zero (open arrow in (a), cf. Fig. 3a) the spectrum also becomes narrow. The parameters are: $J = 1$ (always); $kT = 1$, $h_0 = 0$ in (a); $kT = 1$, $h_0 = 0.8$ in (b); $h_0 = 0.4$, $h = 0.35$ in (c).

Acknowledgements

One of us (UB) is deeply indebted to Péter Szépfalusy for stimulating discussions and for his continuous encouragement and interest over years. Helpful discussions with Tamás Tél are gratefully acknowledged. Thanks is due to Karen Lippert and Dietmar Mülsch for their assistance in preparing the manuscript.

References

1. P. Ruján, *Physica* **91A** (1978) 549.
2. G. Györgyi and P. Ruján, *J. Phys. C* **17** (1984) 4207.
3. T. Nattermann and P. Ruján, *Int. J. Mod. Phys.* **3** (1989) 1597.
4. R. Bruinsma and G. Aeppli, *Phys. Rev. Lett.* **50** (1983) 1494; G. Aeppli and R. Bruinsma, *Phys. Lett.* **97A** (1983) 117.
5. J. M. Normand, M. L. Mehta and H. Orland, *J. Phys.* **A18** (1985) 621.
6. D. Andelmann, *Phys. Rev.* **B34** (1986) 6214.
7. P. Szépfalusy and U. Behn, *Z. Phys.* **B65** (1987) 337.
8. U. Behn and V. A. Zagrebnov, *J. Stat. Phys.* **47** (1987) 939; *J. Phys.* **A21** (1988) 2151; *Phys. Rev.* **B38** (1988) 7115.
9. S. N. Evangelou, *J. Phys. C* **20** (1987) L511.
10. J. Bene and P. Szépfalusy, *Phys. Rev.* **A37** (1988) 1703; J. Bene, *Phys. Rev.* **A39** (1989) 2090.
11. T. Tanaka, H. Fujisaka and M. Inoue, *Phys. Rev.* **A39** (1989) 3170; *Progr. Theor. Phys.* **84** (1990) 584.
12. D. Derrida, J. Vannimenus and Y. Pomeau, *J. Phys. C* **11** (1978) 4749.
13. U. Behn, V. B. Priezzhev and V. A. Zagrebnov, *Physica* **A167** (1990) 457.
14. J. G. Kemeny and J. L. Snell, *Finite Markov Chains* (Springer, Berlin, 1983).
15. T. C. Halsey, M. H. Jensen, L. Kadanoff, I. Procaccia and B. I. Shraiman, *Phys. Rev.* **A33** (1986) 1141.
16. For an introduction see, e.g., Hao Bai-lin, *Elementary Symbolic Dynamics*, (World Scientific, Singapore, 1989).
17. P. Szépfalusy and T. Tél, *Phys. Rev.* **A34** (1986) 2520; T. Tél, *Phys. Lett.* **119A** (1986) 65.
18. T. Tél, *Phys. Rev.* **A36** (1987) 1502; 2507.
19. T. Bohr and T. Tél, in *Directions in Chaos* **2**, ed. Hao Bai-lin (World Scientific, Singapore, 1988); T. Tél, in *Directions in Chaos* **3**, ed. Hao Bai-lin (World Scientific, Singapore, 1990).
20. M. J. Feigenbaum, I. Procaccia and T. Tél, *Phys. Rev.* **A39** (1989) 5359.
21. See, e.g., R. Eykholt and D. K. Umberger, *Phys. Rev. Lett.* **57** (1986) 2333; W. Jeżewski, *Phys. Rev.* **A38** (1988) 3816.
22. A.-L. Barabási, P. Szépfalusy and T. Vicsek, *Physica*A **178** (1991) 17.
23. R. Bruinsma, *Phys. Rev.* **B30** (1984).
24. F. Martinelli and E. Scoppola, *J. Stat. Phys.* **50** (1988) 1021; P. Ruján, *J. Stat. Phys.* **49** (1987) 139; J. L. van Hemmen, G. Keller and R. Kühn, *Europhys. Lett.* **5** (1988) 663.
25. U. Behn, J. L. van Hemmen, R. Kühn, A. Lange and V. A. Zagrebnov, in preparation.